Toxicology Reports 14 (2025) 101909

Contents lists available at ScienceDirect

Toxicology Reports

journal homepage: www.elsevier.com/locate/toxrep

Oxidative damage to DNA, expression of Mt-1, and activation of repair mechanisms induced by vanadium trioxide in cultures of human lymphocytes

V.A. Alcántara-Mejía [a,b], A.A. Beltrán-Flores [a], R.A. Mateos-Nava [a], L. Álvarez-Barrera [a], I.U. Bahena-Ocampo [c], E. Santiago-Osorio [d], E. Bonilla-González [c], J.J. Rodríguez-Mercado [a,*]

[a] Unidad de Investigación en Genética y Toxicología Ambiental, Unidad Multidisciplinaria de Investigación Experimental (UMIE-Z), Facultad de Estudios Superiores-Zaragoza, Campus II, UNAM, Ciudad de México CP 09230, Mexico
[b] Posgrado en Ciencias Biológicas, UNAM, Edificio E, Primer Piso, Circuito de Posgrados, Ciudad Universitaria, Coyoacán, Ciudad de México CP 04510, Mexico
[c] Departamento de Ciencias de la Salud, Universidad Autónoma Metropolitana-Campus Iztapalapa, Ciudad de México CP 09340, Mexico
[d] Unidad de Investigación en Diferenciación Celular y Cáncer, UMIE-Z, Facultad de Estudios Superiores-Zaragoza, Campus II, UNAM, Ciudad de México CP 09230, Mexico

ARTICLE INFO

Handling Editor: Prof. L.H. Lash

Keywords:
Fpg-modified comet assay
Protein expression
QPCR
ATM
BER
NHEJ
V_2O_3

ABSTRACT

Vanadium (V) has garnered attention due to its pharmacological properties; however, its toxic effects have also been documented. Among the vanadium compounds that are found in the environment, vanadium trioxide (V_2O_3) has attracted interest because of its impact on biomolecules such as DNA, RNA, and proteins. However, its precise mechanism of action remains unclear, although it is suspected to be related to oxidative stress. Therefore, this study aimed to determine the mechanisms involved in DNA damage and the associated cellular response pathways. Primary cultures of human lymphocytes were exposed to 2, 4, 8, or 16 μg/mL V_2O_3. DNA damage due to oxidized bases was evaluated via a comet assay. The expression levels of sensor proteins (ATM and ATR) involved in DNA damage were determined via Western blotting, and the mRNA expression levels of metallothionein 1 (*Mt-1*) and genes involved in DNA repair (*OGG1*, *APE1*, *XPB*, *XPD*, *MRE11*, *RAD50*, *Ku70*, and *Ku80*) were estimated via RT-PCR and qPCR. The results showed that V_2O_3 is an oxidant that is responsible for DNA damage through oxidized bases, as demonstrated by increased DNA migration in the presence of the FPG enzyme. At the molecular level, V_2O_3 treatment also increased ATM protein expression. In terms of mRNA expression, the overexpression of *Mt-1*, *OGG1*, *APE1*, *Ku70*, and *Ku80* was observed. This finding suggests that DNA damage is primarily repaired via two mechanisms: base excision repair (BER) and nonhomologous end joining (NHEJ). In conclusion, one mechanism of action of V_2O_3 involves the oxidation of nitrogenous bases in DNA, the activation of damage sensors (such as ATMs), and the overexpression of Mt-1 as part of the antioxidant response to mitigate the effects of V and facilitate DNA repair pathways (including BER and NHEJ).

1. Introduction

Vanadium (V) compounds have attracted considerable interest due to their pharmaceutical applications; however, *in vivo* studies have demonstrated certain toxicities in different organs, depending on the specific chemical compound and oxidation state [1,2].

In the atmosphere, compounds are formed via fossil fuel combustion, with compounds including vanadium oxides such as vanadium pentoxide (V_2O_5), vanadium tetroxide (V_2O_4), and vanadium trioxide (V_2O_3), to which populations are exposed. V_2O_5 accounts for three-quarters of all vanadium oxides; however, industries have strived to minimize its formation because when V_2O_5 comes into contact with sulfur dioxide (SO_2) and moisture, it generates sulfuric acid (H_2SO_4), which is corrosive to combustion machinery [3–5]. This process leads to the formation and release of vanadium in the form of V_2O_4 and V_2O_3.

Vanadium oxides in the air and particulate matter (PM) enter the body via inhalation [6–8] and travel throughout the circulatory system by binding to transferrin or albumin, after which they eventually accumulate in various organs [1,9–11].

It has been reported that V levels in unexposed students range from

* Correspondence to: Facultad de Estudios Superiores-Zaragoza, Campus II, UNAM, Ciudad de México CP 09230, Mexico.
E-mail address: juserom@unam.mx (J.J. Rodríguez-Mercado).

https://doi.org/10.1016/j.toxrep.2025.101909
Received 8 November 2024; Received in revised form 27 December 2024; Accepted 11 January 2025
Available online 13 January 2025

0.01–1.20 ng/mL [12]. In studies comparing blood V levels in children living near metallurgical plants, the median V level was 0.078 μg/L, whereas in children from rural areas, the median V level was 0.042 μg/L [13].

The V levels in the urine and blood of exposed workers have been shown to be 50–2000 times higher, with ranges of 3.1–217 ng/mL in workers compared with 0.02–0.095 ng/mL in the reference group [14], as well as ranges of 3.02–762 ng/mL in workers compared with 0.06–0.48 ng/mL in nonexposed individuals [15]. Additionally, cases of intoxication, exposure due to medical prosthetics, and even death due to ingestion with respect to V have been reported [16–18].

In Mexico, increased V levels have been reported by determining metal concentrations in lung tissues [19] and by measuring vanadium levels in the atmosphere [5,20]. The effects of V_2O_5 are well documented; specifically, this compound is known to induce adenomas and lung carcinomas in mice and is considered to be a possible carcinogen for humans [21]. However, few studies have investigated other oxides, especially V_2O_3.

V_2O_3 is known to induce chromosomal aberrations, sister chromatid exchange, and single-strand breaks, as well as increase the expression of phosphorylated variant histone A (H2AX), which is a marker of double-strand DNA breaks [22–25]. Additionally, it reduces the mRNA expression levels and protein products of cyclin D, cyclin E, cdk2, and cdk4 [25]. These effects may be linked to increased levels of reactive oxygen species, as V_2O_3 exposure in cells elevates hydrogen peroxide (H_2O_2) levels; by participating in the Fenton and Haber-Weiss reactions, increased H_2O_2 levels subsequently generate hydroxyl radicals (·OH) and vanadyl ions (VO^{2+}). This effect can impair the antioxidant defense system, thereby leading to lipid peroxidation, protein oxidation, and damage to the nitrogenous bases of nucleic acids [25–28].

Cells respond to DNA damage in various ways, including the activation of deoxyribonucleic acid (DNA) repair mechanisms, detoxification, senescence, or programmed cell death [7,29]. The cell relies on complex systems that recognize both endogenous and induced damage. The proteins involved in these systems correspondingly activate signaling cascades that include sensor protein complexes such as the MRN complex (meiotic recombination 11, or MRE11; ATP-binding cassette-ATPase, or RAD50; and Nijmegen breakage syndrome 1, or NBS1), Ku protein (Ku70/80) heterodimers, or RPA and the 911 complex (replication protein A and Rad9-Hus1-Rad1), which activate transducers such as Ataxia telangiectasia mutated (ATM) and ATM and Rad3-related (ATR). These transducers subsequently stimulate effectors such as p21, although p53 does not increase in these cases [30–32].

Concrete data regarding the repair mechanisms that are activated in response to the genotoxic damage caused by V_2O_3 are still lacking. However, due to the nature of the lesions that are induced by V_2O_3 [22–26], we suspect that the excision repair machinery (base excision repair [BER] or nucleotide excision repair [NER]) and recombination machinery (homologous recombination [HR] or nonhomologous end joining [NHEJ]) are activated. Furthermore, the response of antioxidant molecules, such as metallothionein 1 (Mt-1) (which protects cells from heavy metal toxicity) [33,34], has also not been sufficiently explored. Therefore, in the current study, we focused on the effects of V_2O_3 in cultures of human lymphocytes with the aim of determining the mechanisms that are involved in DNA damage and the associated cellular response pathways.

Specifically, we evaluated whether V_2O_3 induces changes in the expression of Mt-1, ATM, and ATR; assessed DNA damage via oxidized bases; and analyzed the DNA repair mechanisms that are activated by this damage.

2. Materials and methods

2.1. Reagents

The following reagents were used to develop the protocols: vanadium trioxide (V_2O_3, CAS 1314–34–7 with 99.99 % purity), Histopaque®-1077, phosphate-buffered saline (PBS), agarose, NaCl, Nonidet P-40, DTT (1,4-dithiothreitol), sodium orthovanadate (NaVO4), sodium biphosphate (NaH_2PO_4), disodium phosphate (Na_2HPO_4), Na2-EDTA, Trizma® base, and DMSO, with all of these reagents being obtained from Sigma-Aldrich, Inc., MO, USA. The formamidopyrimidine-DNA glycosylase enzyme (Fpg) was obtained from New England BioLabs® by ChemCruz®, Dallas, USA. PB-MAXTM Karyotyping medium and RPMI-1640 medium were obtained from Gibco BRL-Invitrogen Corporation, NY, USA. Acrylamide, N,N′-methylenebisacrylamide, glycine, sodium dodecyl sulfate (SDS), N,N,N′,N′-tetramethylethylenediamine (TEMED), tris(hydroxymethyl)aminomethane (Tris), ammonium persulfate, and the Bio-Rad protein assay were purchased from Bio-Rad Laboratories, CA, USA. The protease inhibitors aprotinin, leupeptin, and PMSF; the primary antibodies anti-ATM (sc-377293), anti-ATR (sc-515173), and anti-actin (sc-8432); the horseradish peroxidase-conjugated secondary antibody m-IgGk BP-HRP (sc-516102); the goat anti-mouse antibody IgG-HRP and Tween 20; and the Western Blotting Luminol Reagent (sc-2048) were obtained from Santa Cruz Biotechnology, Inc., CA, USA. EDTA was obtained from BD Diagnostics, Mexico. The TRIzol Reagent, RevertAid First Strand cDNA Kit (K-1622), and Maxima SYBR Green/ROX qPCR Master Mix (K-0221) were obtained from Thermo Fisher Scientific, MA, USA; additionally, Crystal Taq Master Mix (2x) was obtained from Jena Bioscience, Germany.

2.2. Lymphocyte culture and treatments

Peripheral blood samples were collected from three volunteers via the Vacutainer® system, and lymphocytes were isolated with Histopaque®-1077. For the single-cell gel electrophoresis assay, 4×10^5 cells were incubated in 3 mL of RPMI-1640 medium supplemented with 2, 4, 8, or 16 μg/mL V_2O_3 for 2 h. V_2O_3 was ground and dissolved in distilled water before use.

For the other assays, 1×10^7 cells were incubated in 5 mL of PB-MAX karyotyping medium for 24 h at 37°C. After this incubation period, V_2O_3 at concentrations of 2, 4, 8, or 16 μg/mL was added, and the cells were incubated for an additional 24 h. An untreated group (0 μg/mL) was included in all of the cases. The utilized concentrations were selected based on previous reports. The procedures involving human volunteers adhered to the guidelines of the Helsinki and Tokyo Declarations and were approved by the Committee of Ethics and Biosecurity of FES-Zaragoza, UNAM (registration number: FESZ-CE/21–118–01).

2.3. Comet assay

After the treatments, the cells were collected via centrifugation, and 40 μL of the cell suspension was mixed with 260 μL of low melting point agarose and placed onto four slides that had been previously coated with a uniform layer of 1 % normal melting point agarose, according to protocols described in previous reports [23]. The preparations were submerged in lysis solution (2.5 M NaCl, 100 mM Na2-EDTA, 10 mM Trizma® base, pH 10, and 1 % Triton X-100) for 24 h at 4°C. Two preparations from each treatment were used for the standard comet assay, and the other two preparations were used for the Fpg enzyme-modified version.

The lysis solution was removed, and half of the preparations were placed into a horizontal electrophoresis chamber (Claver Scientific, CSL-COM Series, Mexico). Electrophoresis was performed by using electrophoresis buffer (300 mM NaOH and 1 mM EDTA, pH > 13) for 20 min at 25 V and 300 mA. The slides were subsequently placed into a neutral solution (0.4 mM Trizma® base, pH 7) for 10 min and fixed with 70 % ethanol for 10 min. The preparations were subsequently stained with 25 μL of ethidium bromide (0.025 μg/mL) and observed under a fluorescence microscope with a green filter (515–560 nm) at 400X magnification. DNA damage was estimated using an ocular micrometer by

measuring the length of the nucleoids in 200 comets per sample, which ultimately resulted in a total of 600 comets per treatment.

2.4. Fpg-modified comet assay

The preparations that were intended for the assessment of DNA damage caused by oxidized bases via the use of the Fpg enzyme were processed as follows. After lysis, the preparations were washed with PBS and then rinsed three times with reaction buffer (40 mM HEPES, 0.1 M KCl, 0.5 mM EDTA, and 0.2 mg/mL BSA at pH 8.0) following the manufacturer's instructions. Subsequently, 50 μL of the diluted enzyme (0.5 UI/mL) was added to each preparation and incubated at 37°C for 20 min. After incubation with Fpg, single-cell gel electrophoresis was performed as previously described, and the comet length data were obtained.

2.5. Analysis of protein expression levels

Proteins were obtained by lysing the cells with RIPA buffer (150 mM NaCl, 5 mM EDTA, 1 % Nonidet P-40, 0.1 % SDS, 1 mM DTT, 1 mM $NaVO_4$, 5 mM Na_2HPO_4, and 10 mM NaH_2PO_4) and protease inhibitors. The protein concentration was determined using the use of the Bio-Rad protein assay reagent. The proteins were subsequently separated via polyacrylamide gel electrophoresis (SDS-PAGE, 12 %) at a constant current of 100 V, after which they were transferred to a Bio-Rad PVDF membrane via electroblotting at a constant current of 145 mA and blocked with 5 % fat-free powdered milk in TBST (0.05 % Tween 20 in Tris-buffered saline). The membrane was subsequently incubated overnight at 4°C with one of the following primary antibodies: anti-ATM, anti-ATR, or anti-actin (with the latter antibody being used as a loading control). The membrane was incubated with the secondary antibody for 90 min, washed, and then incubated with the Western blotting Luminol Reagent. The reaction was captured by using the Bio-Rad ChemiDoc™ MP Imaging System. Band expression was analyzed via ImageJ 1.51d software from the National Institutes of Health, USA (https://imagej.nih.gov/ij/).

2.6. RNA extraction and cDNA synthesis

Total RNA was isolated from 1×10^7 cells via the standard TRIzol extraction method (following the manufacturer's protocol) and resuspended in 40 μL of molecular biology grade water. The purity and quantity of the RNA were determined with a biophotometer (Eppendorf AG 22331), and the RNA integrity was assessed via horizontal electrophoresis on a 1 % low-melting-point agarose gel. The RNA samples were reverse transcribed into cDNA by using 3 μg of total RNA and the RevertAid First Strand cDNA kit (K-1622) with 1 μL of oligo(dT) primer, 4 μL of 5X reaction buffer, 1 μL of RiboLock RNase Inhibitor (20 U/μL), 2 μL of dNTP mixture (10 mM), and 1 μL of RevertAid M-MuLV RT (200 U/μL), for a final volume of 20 μL. The reaction was performed at 42°C for 60 min, followed by 5 min at 70°C. The reaction tubes containing the reverse transcription (RT) preparations were then cooled on ice for subsequent cDNA amplification via PCR.

2.7. Qualitative polymerase chain reaction

The sequences of the specific primers and the product sizes are listed in Table 1. The presence of Mt was assessed via the use of 10 μL of Crystal Taq Master Mix (2x), 0.8 μL of oligos (0.3 μM), 2 μL of cDNA (150 ng), and 7.2 μL of RNase-free water. The reaction was performed in the MiniPCR thermocycler under the following conditions: 95°C for 120 s, 95°C for 15 s, 60°C (or the optimal temperature for each primer) for 30 s, and 72°C for 60 s; the last three steps were repeated for 30 cycles, followed by a final cycle at 72°C for 5 min. The products were loaded onto a 2 % agarose gel along with the products of the constitutive gene. The relative expression intensities of the genes were obtained via the Bio-Rad ChemiDoc™ system.

2.8. Gradient polymerase chain reaction

A mix of cDNA from cultures treated with 0, 2, 4, 8, and 16 μg/mL V_2O_3 was prepared to verify the expression of repair genes (BER, NER, HR, and NHEJ), eliminate nonspecific products, and determine the optimal amplification temperature. The reaction was performed with 10 μL of Crystal Taq Master Mix (2x), 0.8 μL of oligos (0.3 μM), 2 μL of cDNA mixture (400 ng), and 7.2 μL of RNase-free water. The mixture

Table 1
Primer characteristics according to Primer-BLAST.

Gen		Sequence (5′→3′)	Variant	Product	Tm (°C)
β–Actin	F	TTCTACAATGAGCTGCGTGTG	α1, 2, 9, 1, 11, 5, 10, 3, 8, 4, 6, like 2, X1.	122 pb	60
	R	GGGGTGTTGAAGGTCTCAAA			
Mt−1	F	TCTCCTTGCCTCGAAATGGAC	Mt−1X, Mt−1E, Mt−1E "like", Mt−1E V2, Mt−1A, Mt-1M, Mt-1F, Mt-1F V1	151 pb	59
	R	GGGCACACTTGGCACAGC	Mt−1E V1	499 pb	
OGG1	F	ACTCCCACTTCCAAGAGGTG	X8, X7, X6, X5, X4, X3, X2, X1, 2e, 2c, 2 f, 1b, 1a, 2 h, 2d, 1c, 1e, 1d, 2b, 2a, 2 g.	165 pb	58
(BER)	R	GGATGAGCCGAGGTCCAAAAG			
APE1	F	CAATACTGGTCAGCTCCTTCG	2, 4, 3, 1.	88 pb	53
(BER)	R	TGCCGTAAGAAACTTTGAGTGG			
XPD	F	TCTGCCTCTGCCCTATGAT	X2, 1.	363 pb	54
(NER)	R	CGATTCCCTCGGACACTTT	CNOT3 (X16, X54, X52, X29, X28, X24, X16, X21)	1991 pb	
			WIPF1	3893 pb	
XPB	F	CCAGGAAGCGGCACTATGAGG	X2, X1, 1, 2, 3.	171 pb	53
(NER)	R	GGTCGTCCTTCAGCGGCATTT			
Rad50	F	CTTATACAGGACCAGCAGGAAC	Rad50	686 pb	58
(HR)	R	CCTTTCTGTCGCCCTAATGC			
MRE11	F	CCAGAGAGCCCTTGTACG	X10, X9, X7, X5, X4, X1, X10, X9, X7, X5, X4, X1, 1, 3, 2.	667 pb	57
(HR)	R	TTCCACCTCTTCGACCTCTTC	ZBTB4.- X11, X12, X10, X9, X8, X2, X1, X7, X6, X5, X4, X1, X3, X2, 1, 2.	1675 pb	
			FAM120A.- X9, X8, X7, X6, X5, X4, X3, X2, X1.	2737 pb	
			SALL2.- X2, X1, 1, 6,	1543 pb	
			SETD1A.- X6, X5, X4, X2, X3, X1.	949 pb	
			LRRC41	208 pb	
Ku70	F	CCGAGATACAGGCATCTTCCT	X1, 4, 3, 2, 1.	204 pb	54
(NHEJ)	R	AGCTTTAACCTGCTGAGTGCT	PHYKPL.- X7	96 pb	
Ku80	F	AGCATAGACTGCATCCGAGC	1, X1.	315 pb	59
(NHEJ)	R	TCCCCATACATCCACGACCT			

F, Forward; R, Reverse; pb, base pairs; Tm, Melting temperature (°C). The genes were purchased from Alpha DNA, PROBIOTEK.

was placed into the thermocycler under the following conditions: 95°C for 120 s, 95°C for 15 s (with the annealing temperature ranging from 50°C to 62°C for 30 s), and 72°C for 60 s; the last three steps were repeated for 40 cycles, followed by a final cycle at 72°C for 5 min. The products were analyzed in the same manner as for the previous PCR protocol, and product identification was used as the indicator to proceed with qPCR.

2.9. Quantitative polymerase chain reaction (qPCR)

qPCR was performed for the excision and recombination repair genes via the use of 10 μL of Maxima SYBR Green/ROX qPCR Master Mix (2X), 0.8 μL of oligos (0.3 μM), 2 μL of cDNA (150 ng), and 7.2 μL of RNase-free water. The reaction was performed in a 7500 Real-Time PCR System under the following conditions: 95°C for 120 s, 95°C for 15 s, 60°C (or the optimal temperature for each primer) for 30 s, and 72°C for 60 s. The last three steps were repeated for 40 cycles, followed by a final cycle at 72°C for 5 min. The same reaction conditions were used for the other genes.

2.10. Statistical analyses

The data were analyzed using Prism 9.0.1 software for Mac. Normality was assessed with the Shapiro-Wilk and Kolmogorov-Smirnov tests. For normally distributed data, the results are presented as the mean ± standard error of the mean (SEM). For nonnormally distributed data, the results are expressed as the median and the interquartile range (IQR), represented by the first (Q1) and third (Q3) quartiles. For all of the experiments, three independent experiments were performed, with each experiment performed in duplicate (n = 6). To determine significant differences between the treated and untreated groups, analysis of variance (ANOVA) or Kruskal-Wallis tests were applied, with post hoc Tukey (equal variances), Dunnett (unequal variances), or Bonferroni correction (to adjust for p value calculation error) tests being conducted. Furthermore, * $p < 0.05$ and * * $p < 0.01$ were considered to indicate statistical significance.

3. Results

3.1. Assessment of DNA damage

When comparing the results of those untreated and treated with V_2O_3 increased the comet length samples, thus indicating the presence of DNA damage (Fig. 1a). When the Fpg enzyme was used, a greater increase was observed, thereby suggesting that the DNA damage was partially due to the presence of oxidized bases (Fig. 1b). A comparison of the comet length data from cells without Fpg (-) and with Fpg (+) revealed that oxidative DNA damage occurred in a concentration-dependent manner in response to V_2O_3 (Fig. 1c).

3.2. Mt-1 Activation

Compared with those in untreated cells, V_2O_3-treated cells for 24 h in the 4, 8, and 16 μg/mL groups presented upregulated expression (Fig. 2).

3.3. Expression levels of DNA damage sensor proteins

V_2O_3 administration for 24 h promoted ATM protein expression, with significant differences being observed at concentrations of 2 and

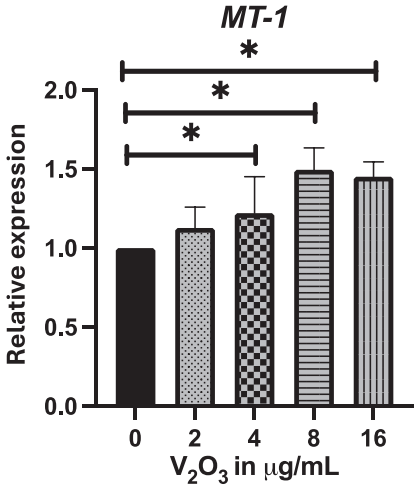

Fig. 2. *Mt-1* mRNA expression. Relative expression levels of *Mt-1* mRNA in human lymphocyte cultures that were untreated (0 μg/mL) or treated with 2, 4, 8, or 16 μg/mL V_2O_3 for 24 h. The data are presented as the means ± SEMs from three independent experiments, with each experiment performed in duplicate (n = 6). * $p < 0.05$ vs. the untreated group (ANOVA-Tukey test).

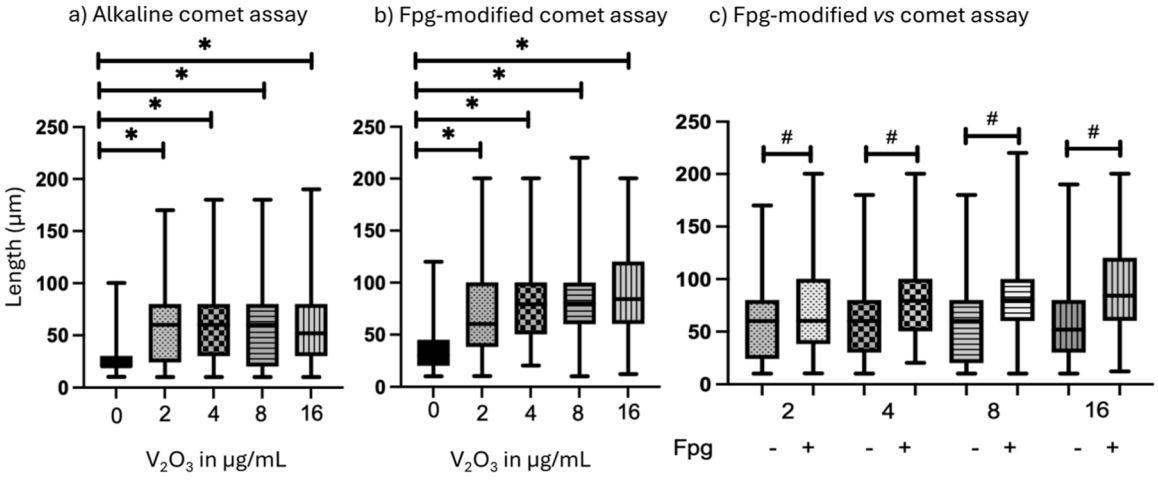

Fig. 1. Comet assay to assess oxidative DNA base damage. Comet length in human lymphocyte cultures that were untreated (0 μg/mL) or treated with 2, 4, 8, or 16 μg/mL V_2O_3 for 2 h. a) Alkaline comet assay; b) alkaline comet assay with the formamidopyrimidine-DNA glycosylase (Fpg) enzyme; c) comparison of treatments without (-) and with (+) the Fpg enzyme. Data are presented as medians, with the box extending from Q1 to Q3. * $p < 0.05$ vs. the untreated group. # $p < 0.05$ vs. the respective Fpg (-) group (Kruskal-Wallis test with Bonferroni correction for multiple comparisons).

16 μg/mL. In contrast, the ATR results did not significantly change (Fig. 3 and supplementary material A1).

3.4. mRNA expression levels of genes involved in DNA repair mechanisms

The expression of two genes per repair mechanism was evaluated, including 8-oxoguanine DNA glycosylase 1 (*OGG1*) and apurinic/apyrimidinic endonuclease 1 (*APE1*) for BER, Xeroderma pigmentosum group B (*XPB*) and Xeroderma pigmentosum group D (*XPD*) for NER, *MRE11* and *RAD50* for HR, and *Ku70* and *Ku80* for NHEJ, which are representative genes for each mechanism. The optimal annealing and amplification temperatures for each gene were determined via gradient PCR within a temperature range of 50–62°C, which was then used for qPCR.

The results of the gradient PCR analysis demonstrated that the HR repair mechanism was not activated, as *MRE11* and *RAD50* were not detected (A2), which differed compared to the expression of other genes, such as Ku80, in which nonspecific amplification was observed at lower temperatures (except at 59.3°C) (A3).

The $2^{-\Delta\Delta Ct}$ method was used with β-actin as the reference, and the calibration curve (R^2: 0.977) and Ct for each concentration (A4) were obtained. The qPCR results for *OGG1* demonstrated increases at all concentrations, with significant differences observed at 4, 8, and 16 μg/mL V_2O_3; moreover, the results for *APE1* demonstrated increases at 8 and 16 μg/mL V_2O_3 (Fig. 4). For the helicases *XPB* and *XPD* (Fig. 5), no significant changes were observed compared with those in the control. However, increases ($p < 0.05$) in *Ku70* and *Ku80* expression were observed at 4, 8, and 16 μg/mL V_2O_3 (Fig. 6).

4. Discussion

The primary chemical form of V that is released during the combustion of fossil fuels is V_2O_5 [3–5]. However, under certain atmospheric conditions, V transforms into V_2O_3 [35], thus highlighting the importance of investigating the mechanisms by which V induces its toxicity.

The genotoxicity of V compounds has been demonstrated in cell lines and human leukocytes via the comet assay. The increase in comet tail length can reveal various types of lesions, including single-strand breaks, double-strand breaks, AP sites, and incomplete repair sites in DNA [23,36,37], which aligns with the results of this study. Additionally, the Fpg-modified comet assay revealed that some of the DNA damage induced by V_2O_3 treatment was due to oxidative stress. Fpg recognizes oxidized bases and cleaves the glycosidic bond, thereby resulting in AP sites; under alkaline conditions of electrophoresis, AP sites are converted to single-strand breaks. This increases the degree of observed DNA damage, which is reflected as longer comet tails than those evaluated without the use of the enzyme. This effect is comparable to that reported in workers and experimental mouse models exposed to V_2O_5, wherein oxidized bases were detected via the comet assay [38] and high-performance liquid chromatography [39]. V_2O_3 also increases H_2O_2 levels [25,40], which is a substrate for the metal to generate ·OH

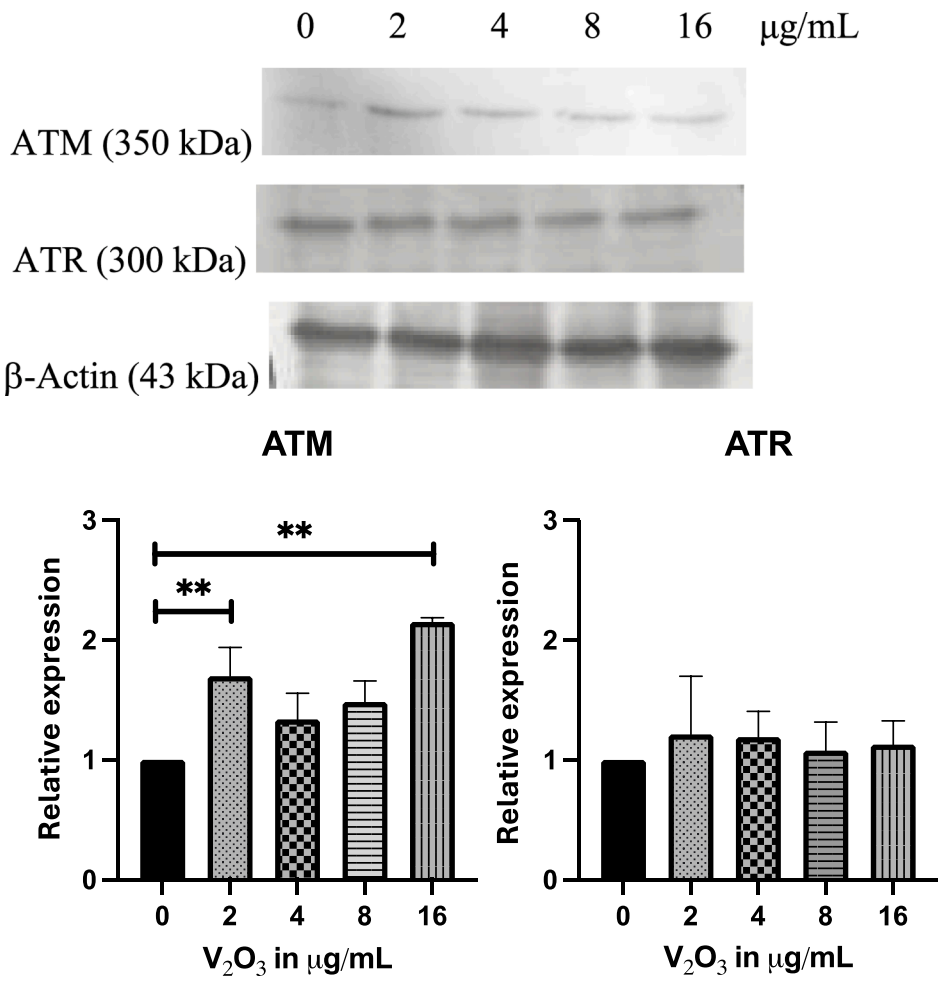

Fig. 3. DNA damage sensors induced by V_2O_3. Relative protein expression levels of ATM and ATR in human lymphocyte cultures that were untreated (0 μg/mL) or treated with 2, 4, 8, or 16 μg/mL V_2O_3 for 24 h. The data are presented as the means ± SEMs from three independent experiments, with each experiment performed in duplicate (n = 6). * * $p < 0.01$ vs. the untreated group (ANOVA-Tukey test).

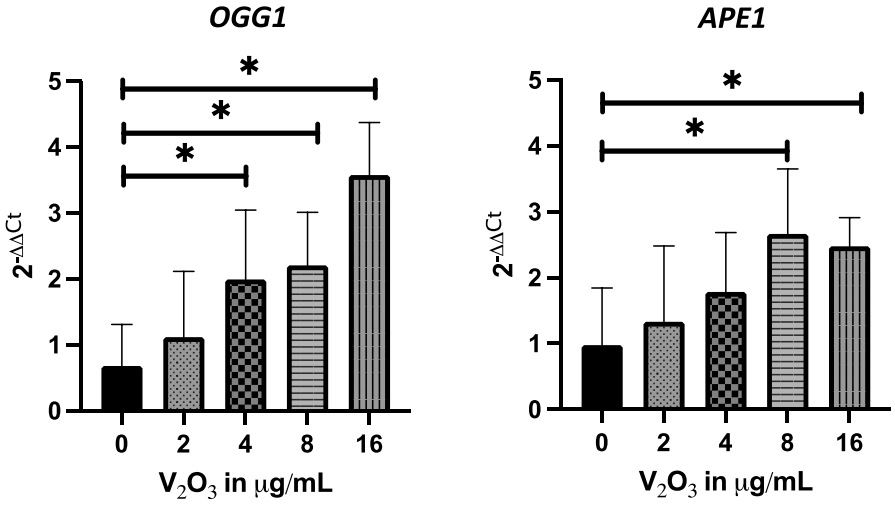

Fig. 4. Gene expression levels involved in the BER pathway. $2^{-\Delta\Delta Ct}$ of *OGG1* and *APE1* mRNA in human lymphocyte cultures, that were untreated (0 μg/mL) or treated with 2, 4, 8, or 16 μg/mL V_2O_3 for 24 h. The data are presented as the means ± SEMs from three independent experiments, with each experiment performed in duplicate (n = 6). * $p < 0.05$ vs. the untreated group (ANOVA-Tukey test).

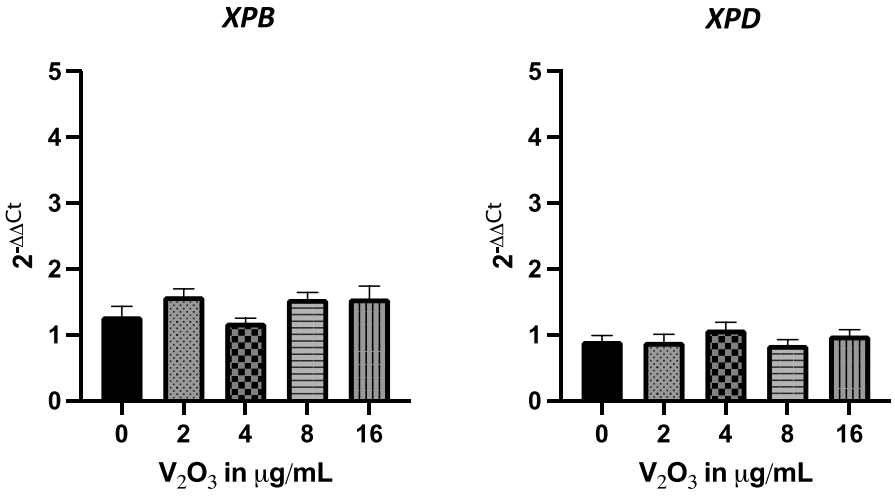

Fig. 5. Gene expression levels involved in the NER pathway. $2^{-\Delta\Delta Ct}$ of *XPB* and *XPD* mRNA in human lymphocyte cultures that were untreated (0 μg/mL) or treated with 2, 4, 8, or 16 μg/mL V_2O_3 for 24 h. The data are presented as the means ± SEMs from three independent experiments, with each experiment performed in duplicate (n = 6). * $p < 0.05$ vs. the untreated group (ANOVA-Tukey test).

[26,41,42], thus leading to oxidative lesions in the nitrogenous bases of DNA.

Mt are proteins that bind to transition metals such as Cu, Zn, Cd, Au, and Hg. The results of previous studies suggest that these proteins also bind to V_2O_3 and other V compounds in the V^{+5} oxidation state, wherein these biomolecules counteract the effects of heavy metals within the cell [43–46]. The increase in Mt-1 mRNA expression may be due to the binding of V^{3+} ions with the metal regulatory transcription factor 1 (MTF-1), which facilitates the binding of RNA polymerase to the promoter region known as the metal response element (MRE), as observed with divalent cations such as Cd and other cations such as Tl [47–49]. Oxidative stress induction can activate a promoter known as the antioxidant response element (ARE) to stimulate the transcription of genes associated with antioxidant defense, including Mt-1 [50]. In this context, our previous studies revealed that V^{3+} increases the generation of reactive oxygen species [25], which may further contribute to the overexpression of Mt-1, thereby activating a protective mechanism to trap the metal and reduce oxidative stress.

The increase in ATM protein levels supports the hypothesis that V_2O_3 induces double-strand DNA breaks, which is consistent with the phosphorylation of the H2AX protein that has been previously reported in response to single-strand breaks and double-strand DNA breaks [23,25,51–53]. The activation of ATM suggests that V_2O_3 affects euchromatic regions of the genome, thereby facilitating chromatin relaxation via KRAB-associated protein 1 (KAP1) phosphorylation to allow for DNA repair; in contrast, repair in heterochromatic regions relies on p53-binding protein 1 (53BP1) [54,55].

The interference of V with essential cofactors such as Cu, Mn, and Zn, which are involved in polymerase function, may be a key factor in generating double-strand DNA breaks [34,37,39,56]. Additionally, increased Mt-1 expression may sequester these metals. Moreover, the resolution of abnormal structures in replication forks or mismatch repair (MMR) processes may lead to the formation of double-strand DNA breaks [57–59].

It has been proposed that unrepaired single-strand breaks, AP sites, or incomplete repair sites that are located within a proximity of 20 bp

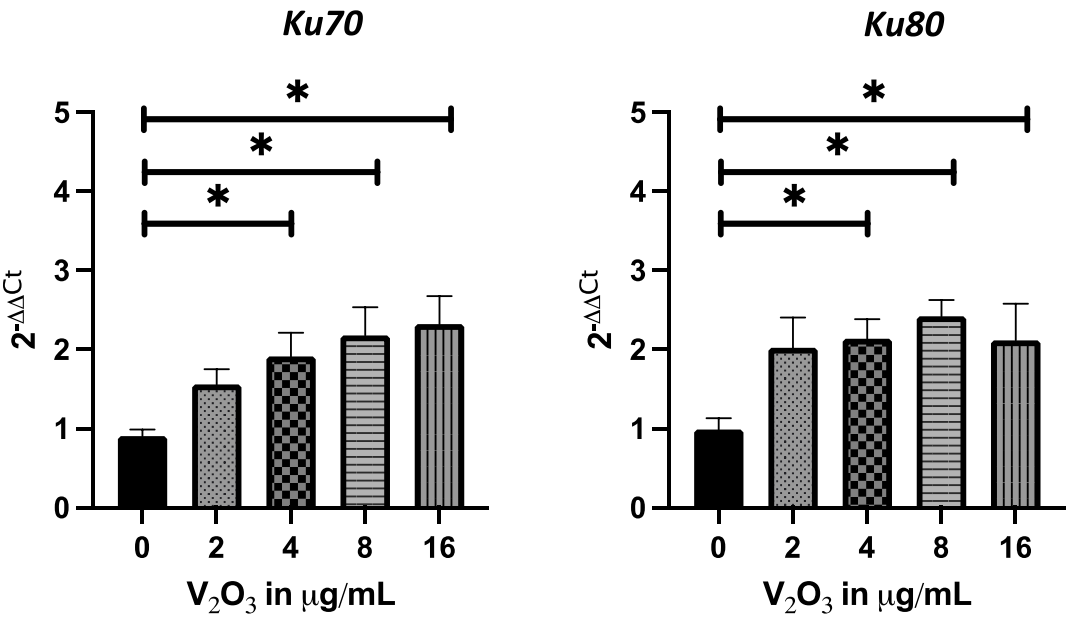

Fig. 6. Gene expression levels involved in the NHEJ pathway. $2^{-\Delta\Delta Ct}$ of *Ku70* and *Ku80* mRNA in human lymphocyte cultures that were untreated (0 μg/mL) or treated with 2, 4, 8, or 16 μg/mL V_2O_3 for 24 h. The data are presented as the means ± SEMs from three independent experiments, with each experiment performed in duplicate (n = 6). * $p < 0.05$ vs. the untreated group (ANOVA-Tukey test).

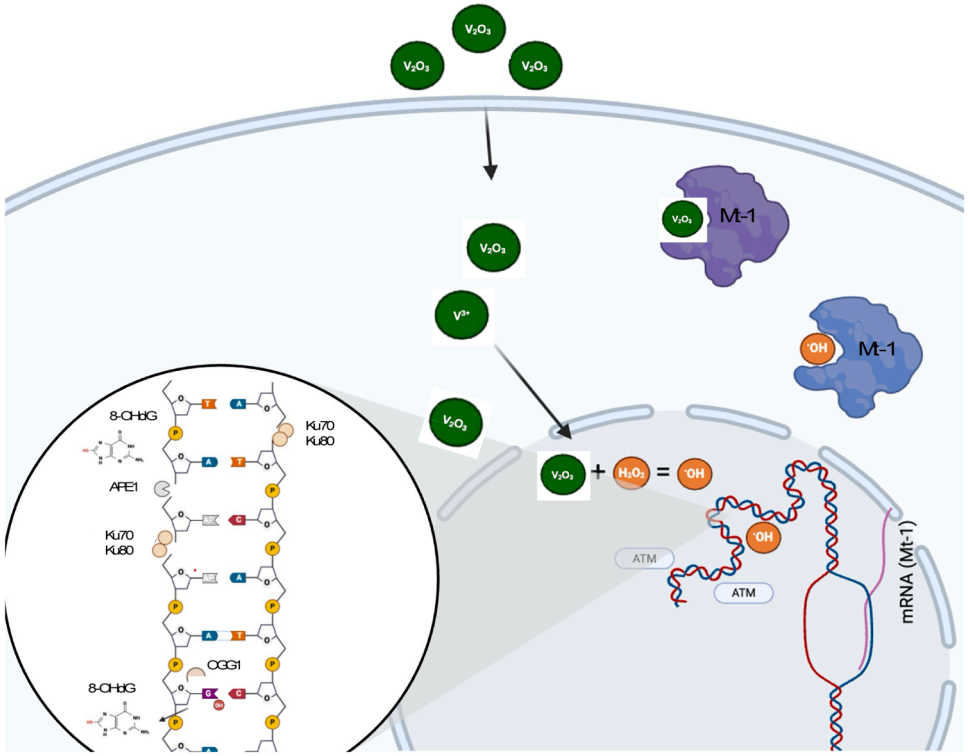

Fig. 7. Schematic diagram of the mechanisms underlying DNA damage and repair in human lymphocytes treated with V_2O_3. Vanadium enters the cell and is distributed to the nucleus, whereas other molecules are sequestered by metallothioneins (such as Mt-1). V_2O_3 molecules and their ions (V^{3+}), which remain free, react with hydrogen peroxide (H_2O_2), thus forming hydroxyl radicals (·OH), which oxidize DNA and cause nitrogenous base oxidation, with 8-hydroxy-2′-deoxyguanosine (8-OHdG) being the primary product. This oxidative damage along the DNA strand is detected by the ATM protein. Free radicals and reactive products, in conjunction with V molecules, can be counteracted by Mt-1. The inset highlights the damage to the DNA molecule that is caused by reactive oxygen species, including AP sites, base oxidation, and single-strand breaks. The cell responds to this damage via the BER machinery, which involves OGG1 glycosylase and APE1 endonuclease, as well as the NHEJ system via the Ku70/80 complex, which recognizes double-strand breaks in the DNA.

may be detected as double-strand DNA breaks by using proteins such as ATM [60]. Despite the presence of damage, V_2O_3 concentrations do not compromise cell viability, thus suggesting that cells may "detoxify" and effectively repair DNA damage.

This study provides evidence of the DNA repair mechanisms triggered by V, specifically with respect to V_2O_3, which induces oxidative base damage. This type of damage activates the BER pathway, as demonstrated by *OGG1* and *APE1* expression; these genes are involved in correcting lesions by excising bases and cleaving phosphodiester bonds, respectively, which is likely a result of oxidative stress.

Metals such as lead (Pb) and arsenic (As) induce similar repair responses, which are reflected by increases in *APE1* expression and 8-hydroxy-2′-deoxyguanosine (8-OHdG) levels [61,62]. Notably, *APE1* not only plays a role in BER but also may participate in the NHEJ pathway [63]. Our findings support this theory by demonstrating increased expression levels of *Ku80* (*XRCC5*) and *Ku70* (*XRCC6*), which are key changes for activating NHEJ; moreover, these changes in expression are correlated with ATM expression and elevated *XRCC4* levels following V exposure [64]. Notably, NHEJ repair is typically activated during the G_1/S phase, which is consistent with our previous findings that V_2O_3 causes cell cycle delays at these phases [25].

The results suggest that V_2O_3 treatments enable cells to repair DNA damage, such as the effects of other metals wherein concentrations in the μM range, such as nickel(II) chloride ($NiCl_2$, 100 μM), favor damage resolution via HR; in contrast, arsenic(III) oxide (As_2O_3, 1–5 μM) primarily leads to damage resolution via the NHEJ pathway [65]. In contrast, the mM concentration level inhibited repair mechanisms, as demonstrated with cadmium (Cd) and copper (Cu) [66].

To summarize, the results of this study showed that V_2O_3 treatment induced Mt-1 expression as part of the detoxification and antioxidant response to mitigate the effects of the metal, as well as those effects generated by reactive oxygen species. This compound causes DNA damage, which is primarily achieved through the oxidation of bases; this damage subsequently activates the BER and NHEJ repair mechanisms (Fig. 7).

5. Conclusions

Our data demonstrate that V_2O_3 treatment induces DNA damage via the oxidation of bases, which subsequently activates DNA repair mechanisms, including BER and NHEJ. Moreover, this damage leads to the upregulation of Mt-1 mRNA expression and ATM protein levels, which are components of the cellular detoxification and antioxidant response aimed at mitigating the oxidative stress generated by V_2O_3. These changes ultimately counteract the genotoxic effects. Nevertheless, due to the fact that each chemical species exerts individual effects, more information on the effects of V compounds will provide greater knowledge of the mechanism of action of V.

Funding

This work was supported by the Universidad Nacional Autónoma de México project PAPIIT IN210324.

CRediT authorship contribution statement

I.U. Bahena-Ocampo: Methodology, Investigation, Formal analysis. **R.A. Mateos-Nava:** Visualization, Supervision, Methodology. **L. Álvarez-Barrera:** Visualization, Resources, Methodology. **V.A. Alcántara-Mejía:** Writing – review & editing, Writing – original draft, Software, Resources, Methodology, Investigation, Formal analysis, Data curation, Conceptualization. **A.A. Beltrán-Flores:** Validation, Methodology, Investigation. **J. J. Rodríguez Mercado:** Writing – review & editing, Writing – original draft, Project administration, Investigation, Funding acquisition, Formal analysis, Data curation, Conceptualization. **E. Santiago-Osorio:** Validation, Supervision, Formal analysis. **E. Bonilla-González:** Validation, Supervision, Formal analysis.

Declaration of Competing Interest

The authors declare that they have no known competing financial interests or personal relationships that could have influenced the work reported in this paper.

Acknowledgments

VA Alcántara-Mejía thanks the Posgrado en Ciencias Biológicas, UNAM, and CONAHCYT for providing scholarship (No. 927419). This work fulfills part of the requirements for obtaining a Doctoral degree at the Posgrado en Ciencias Biológicas, UNAM.

Appendix A. Supporting information

Supplementary data associated with this article can be found in the online version at doi:10.1016/j.toxrep.2025.101909.

Data availability

Data will be made available on request.

References

[1] J.C. Pessoa, S. Etcheverry, D. Gambino, Vanadium compounds in medicine, Coord. Chem. Rev. 301 (2015) 24–48, https://doi.org/10.1016/j.ccr.2014.12.002.
[2] A. Ścibior, J. Kurus, Vanadium and oxidative stress markers - in vivo model: a review, Curr. Med. Chem. 26 (2019) 5456–5500. ⟨https://doi.org/10.2174/0929867326666190108112255⟩.
[3] J.P. Gustafsson, Vanadium geochemistry in the biogeosphere –speciation, solid-solution interactions, and ecotoxicity, Appl. Geochem. 102 (2019) 1–25, https://doi.org/10.1016/j.apgeochem.2018.12.027.
[4] X. Bai, L. Luo, H. Tian, S. Liu, Y. Hao, S. Zhao, S. Lin, C. Zhu, Z. Guo, Y. Lv, Atmospheric vanadium emission inventory from both anthropogenic and natural sources in China, Environ. Sci. 55 (2021) 11568–11578, https://doi.org/10.1021/acs.est.1c04766.
[5] M. Rojas-Lemus, N. López-Valdez, P. Bizarro-Nevares, A. González-Villalva, T. I. Fortoul, Vanadio: exposición atmosférica, efectos en la salud y normatividad en México, Rev. Int. Contam. Ambient. 40 (2024) 181–191, https://doi.org/10.20937/RICA.54869.
[6] B.Y. Niu, W.K. Li, J.S. Li, Q.H. Hong, S. Khodahemmati, J.F. Gao, Z.X. Zhou, Effects of DNA damage and oxidative stress in human bronchial epithelial cells exposed to PM2.5 from Beijing, China, in winter, Int. J. Environ. Res. Public. Health (13) (2020) 4874, https://doi.org/10.3390/ijerph17134874.
[7] X. He, Z.R. Jarrell, Y. Liang, S.M. Ryan, M.L. Orr, L. Marts, Y.M. Go, D.P. Jones, Vanadium pentoxide induced oxidative stress and cellular senescence in human lung fibroblasts, Redox Biol. 55 (2022) 102409, https://doi.org/10.1016/j.redox.2022.102409.
[8] J.B. Li, D. Li, Y.Y. Liu, A. Cao, H. Wang, Cytotoxicity of vanadium dioxide nanoparticles to human embryonic kidney cell line: compared with vanadium (IV/V) ions, Environ. Toxicol. Pharmacol. 106 (2024) 104378, https://doi.org/10.1016/j.etap.2024.104378.
[9] A.R. Byrne, L. Kosta, Vanadium in foods and in human body fluids and tissues, Sci. Total Environ. 10 (1978) 17–30, https://doi.org/10.1016/0048-9697(78)90046-3.
[10] R.J. French, J.H. Jones, Role of vanadium in nutrition: metabolism, essentiality and dietary considerations, Lif. Sci. 52 (1993) 339–346, https://doi.org/10.1016/0024-3205(93)90146-t.
[11] G. Heinemann, B. Fichtl, W. Vogt, Pharmacokinetics of vanadium in humans after intravenous administration of a vanadium containing albumin solution, J. Clin. Pharmacol. 55 (2003) 241–245, https://doi.org/10.1046/j.1365-2125.2003.01711.x.
[12] T.S. Lin, C.L. Chang, F.M. Shen, Whole blood vanadium in Taiwanese college students, Bull. Environ. Contam. Toxicol. 73 (2004) 781–786, https://doi.org/10.1007/s00128-004-0495-9.
[13] J. Kucera, A.R. Byrne, A. Mravcová, J. Lener, Vanadium levels in hair and blood of normal and exposed persons, Sci. Total Environ. (3) (1992) 191–205, https://doi.org/10.1016/0048-9697(92)90329-Q.
[14] J. Kucera, J. Lener, J. Mňuková, Vanadium levels in urine and cystine levels in fingernails and hair of exposed and normal persons, in: J. Kučera, I. Obrusník, E. Sabbioni (Eds.), Nuclear Analytical Methods in the Life Sciences, Humana Press, Totowa, NJ, 1994, https://doi.org/10.1007/978-1-4757-6025-5_39.
[15] J. Kucera, J. Lener, J. Mnukova, E. Bayerová, Vanadium exposure tests in humans: Hair, nails, blood, and urine. Vanadium in the environment. Part 2, John Wiley and Sons, 1998, pp. 55–73. ISBN 9780471177760.

[16] B. Boulassel, N. Sadeg, O. Roussel, M. Perrin, H. Belhadj-Tahar, Fatal poisoning by vanadium, Forensic Sci. Int. 206 (2011) e79–e81, https://doi.org/10.1016/j.forsciint.2010.10.027.

[17] B. Moretti, V. Pesce, G. Maccagnano, G. Vicenti, P. Lovreglio, L. Soleo, P. Apostoli, Peripheral neuropathy after hip replacement failure: is vanadium the culprit? Lancet 379 (2012) 1676, https://doi.org/10.1016/S0140-6736(12)60273-6.

[18] Y.J. Chao, P.T. Lai, Y.T. Lai, C.J. Chao, Severe chemical pneumonitis by vanadium pentoxide responded well to aggressive steroid therapy, Respir. Med. Case Rep. 48 (2024) 102003, https://doi.org/10.1016/j.rmcr.2024.102003.

[19] T.I. Fortoul, A. Quan-Torres, I. Sanchez, I.E. Lopez, P. Bizarro, M.L. Mendoza, L. S. Osorio, G. Espejel-Maya, M.C. Avila-Casado, M.R. Avila-Costa, L. Colin-Barenque, D.N. Villanueva, G. Olaiz-Fernandez, Vanadium in ambient air: concentrations in lung tissue from autopsies of Mexico City residents in the 1960s and 1990s, Arch. Environ. Health 57 (2002) 446–449, https://doi.org/10.1080/00039890209601436.

[20] M.E. Gutiérrez-Castillo, D.A. Roubicek, M.E. Cebrián-García, A. Vizcaya-Ruiz, M. Sordo-Cedeño, P. Ostrosky-Wegman, Effect of chemical composition on the induction of DNA damage by urban airborne particulate matter, Environ. Mol. Mutagen. 47 (2006) 199–211, https://doi.org/10.1002/em.20186.

[21] IARC (International Agency for Research on Cancer), Cobalt in Hard Metals and Cobalt Sulfate, Gallium Arsenide, Indium Phosphide and Vanadium Pentoxide Series, 86, World Health Organization, Lyon, France, 2006.

[22] J. Owusu-Yaw, M.D. Cohen, S.Y. Fernando, C.I. Wei, An assessment of the genotoxicity of vanadium, Toxicol. Lett. 50 (1990) 327–336, https://doi.org/10.1016/0378-4274(90)90026-i.

[23] J.J. Rodriguez-Mercado, R.A. Mateos-Nava, M.A. Altamirano-Lozano, DNA damage induction in human cells exposed to vanadium oxides in vitro, Toxicol Vitro 25 (2011) 1996–2002, https://doi.org/10.1016/j.tiv.2011.07.009.

[24] L. Álvarez-Barrera, J.J. Rodríguez-Mercado, R.A. Mateos-Nava, A. Acosta-San Juan, M.A. Altamirano-Lozano, Cytogenetic damage by vanadium(IV) and vanadium(III) on the bone marrow of mice, Drug Chem. Toxicol. 47 (2024) 721–728, https://doi.org/10.1080/01480545.2023.2263669.

[25] V.A. Alcántara-Mejía, J.J. Rodríguez-Mercado, R.A. Mateos-Nava, L. Álvarez-Barrera, E. Santiago-Osorio, E. Bonilla-González, M.A. Altamirano-Lozano, Oxidative damage and cell cycle delay induced by vanadium(III) in human peripheral blood cells, Toxicol. Rep. 13 (2024) 101695, https://doi.org/10.1016/j.toxrep.2024.101695.

[26] G. Du, J.H. Espenson, Oxidation of vanadium(III) by hydrogen peroxide and the oxomonoperoxo vanadium(V) ion in acidic solutions: a kinetics and simulation study, Inorg. Chem. 44 (2005) 5514–5522, https://doi.org/10.1021/ic050502j.

[27] A. Ścibior, J. Kurus, Vanadium and oxidative stress markers - in vivo model: a review, Curr. Med. Chem. 26 (2019) 5456–5500, https://doi.org/10.2174/0929867326666190108112255.

[28] M. Rojas-Lemus, P. Bizarro-Nevares, N. López-Valdez, A. González-Villalva, G. Guerrero-Palomo, M. Cervantes-Valencia, T.I. Fortoul-van der Goes, Oxidative Stress and Vanadium, IntechOpen, 2021, https://doi.org/10.5772/intechopen.90861.

[29] J.L. Ingram, A. Antao-Menezes, E.A. Turpin, D.G. Wallace, J.B. Mangum, L.J. Pluta, R.S. Thomas, J.C. Bonner, Genomic analysis of human lung fibroblasts exposed to vanadium pentoxide to identify candidate genes for occupational bronchitis, Resp. Res. 8 (2007) 1–13, https://doi.org/10.1186/1465-9921-8-34.

[30] A.N. Blackford, S.P. Jackson, ATM, ATR, and DNA-PK: the trinity at the heart of the DNA damage response, Mol. Cell. 66 (2017) 801–817, https://doi.org/10.1016/j.molcel.2017.05.015.

[31] R.M. Williams, X. Zhang, Roles of ATM and ATR in DNA double strand breaks and replication stress, Prog. Biophys. Mol. Biol. 161 (2021) 27–38, https://doi.org/10.1016/j.pbiomolbio.2020.11.005.

[32] R.A. Mateos-Nava, J.J. Rodríguez-Mercado, L. Álvarez-Barrera, M.C. García-Rodríguez, M.A. Altamirano-Lozano, Vanadium oxides modify the expression levels of the p21, p53, and Cdc25C proteins in human lymphocytes treated in vitro, Environ. Toxicol. 36 (2021) 1536–1543, https://doi.org/10.1002/tox.23150.

[33] N. Thirumoorthy, K.M. Kumar, A.S. Sundar, L. Panayappan, M. Chatterjee, Metallothionein: an overview, World J. Gastroenterol.: WJG 13 (2007) 993–996, https://doi.org/10.3748/wjg.v13.i7.993.

[34] R. Yang, D. Roshani, B. Gao, P. Li, N. Shang, Metallothionein: a comprehensive review of its classification, structure, biological functions, and applications, Antioxidants 13 (2024) 825, https://doi.org/10.3390/antiox13070825.

[35] H. Sicius, Vanadium Group: Elements of the Fifth Subgroup. Handbook of the Chemical Elements, Springer, 2024, pp. 544–547. ISBN 9783662689219.

[36] M. Caicedo, J.J. Jacobs, A. Reddy, N.J. Hallab, Analysis of metal ion- induced DNA damage, apoptosis, and necrosis in human (Jurkat) T-cells demonstrates Ni2+ and V3+ are more toxic than other metals: Al3+ , Be2+ , Co2+ , Cr3+ , Cu2+ , Fe3+ , Mo5+ , Nb5+ , Zr2+, J. Biomed. Mater. Res. A 86 (2007) 905–913, https://doi.org/10.1002/jbm.a.31789.

[37] P. Nunes, Y. Yildizhan, Z. Adiguzel Z, F. Marques, J. Costa Pessoa, C. Acilan, I. Correia, Copper(II) and oxidovanadium(IV) complexes of chromone schiff bases as potential anticancer agents, J. Biol. Inorg. Chem. 27 (2022) 89–109, https://doi.org/10.1007/s00775-021-01913-4.

[38] V.A. Ehrlich, A.K. Nersesyan, C. Hoelzl, F. Ferk, J. Bichler, E. Valic, S. Knasmuller, Inhalative exposure to vanadium pentoxide causes DNA damage in workers: results of a multiple end point study, Environ. Health Perspect. 116 (2008) 1689–1693, https://doi.org/10.1289/ehp.11438.

[39] D. Schuler, H.J. Chevalier, M. Merker, K. Morgenthal, J.L. Ravanat, P. Sagelsdorff, D. McGregor, First steps towards an understanding of a mode of carcinogenic action for vanadium pentoxide, J. Toxicol. Pathol. 24 (2011) 149–162, https://doi.org/10.1293/tox.24.149.

[40] H.A. Ngwa, A. Kanthasamy, V. Anantharam, C. Song, T. Witte, R. Houk, A. G. Kanthasamy, Vanadium induces dopaminergic neurotoxicity via protein kinase Cdelta dependent oxidative signaling mechanisms: relevance to etiopathogenesis of Parkinson's disease, Toxicol. Appl. Pharma. 240 (2009) 273–285, https://doi.org/10.1016/j.taap.2009.07.025.

[41] D.R. Lloyd, P.L. Carmichael, D.H. Phillips, Comparison of the formation of 8-hydroxy-2 '-deoxyguanosine and single-and double-strand breaks in DNA mediated by fenton reactions, Chem. Res. Toxicol. 11 (1998) 420–427, https://doi.org/10.1021/tx970156l.

[42] H. Fickl, A.J. Theron, H. Grimmer, J. Oommen, G.J. Ramafi, H.C. Steel, S.S. Visser, R. Anderson, Vanadium promotes hydroxyl radical formation by activated human neutrophils, Free Radic. Biol. Med. 40 (2006) 146–155, https://doi.org/10.1016/j, freeradbiomed.2005.09.019.

[43] T. Chakraborty, S. Samanta, B. Ghosh, N. Thirumoorthy, M. Chatterjee, Vanadium induces apoptosis and modulates the expressions of metallothionein, Ki-67 nuclear antigen, and p53 during 2-acetylaminofluorene-induced rat liver preneoplasia, J. Cell. Biochem. 94 (2005) 744–762, https://doi.org/10.1002/jcb.20304.

[44] K. Kobayashi, S. Himeno, M. Satoh, J. Kuroda, N. Shibata, Y. Seko, T. Hasegawa, Pentavalent vanadium induces hepatic metallothionein through interleukin-6-dependent and-independent mechanisms, Toxicology 228 (2006) 162–170, https://doi.org/10.1016/j.tox.2006.08.022.

[45] K. Mosna, K. Jurczak, A. Krężel, Differentiated Zn(II) binding affinities in animal, plant, and bacterial metallothioneins define their zinc buffering capacity at physiological pZn, Metallomics 15 (2023) mfad061, https://doi.org/10.1093/mtomcs/mfad061.

[46] D. Juárez-Rebollar, M. Méndez-Armenta, Aspectos funcionales de la metalotioneina en el sistema nervioso central, Arch. Neurocien. 19 (2014) 34–41.

[47] X.L. Chang, T.Y. Jin, Y.F. Zhou, Metallothionein 1 isoform gene expression induced by cadmium in human peripheral blood lymphocytes, Biomed. Environ. Sci. 19 (2006) 104–109.

[48] R. Shimoda, T. Nagamine, H. Takagi, M. Mori, M.P. Waalkes, Induction of apoptosis in cells by cadmium: quantitative negative correlation between basal or induced metallothionein concentration and apoptotic rate, Toxicol. Sci. 64 (2001) 208–215, https://doi.org/10.1093/toxsci/64.2.208.

[49] G.A. Kılıç, M. Kutlu, Effects of exogenous metallothionein against thallium-induced oxidative stress in rat liver, Food Chem. Toxicol. 48 (2010) 980–987, https://doi.org/10.1016/j.fct.2010.01.013.

[50] P. Dziegiel, B. Pula, C. Kobierzycki, M. Stasiolek, Podhorska-Okolow, P. Dziegiel, M. Podhorska-Okolow, Metallothioneins in normal and cancer cells, Adv. Anat. Embryol. Cell. Biol. 218 (2016) 1–117, https://doi.org/10.1007/978-3-319-27472-0_1.

[51] M. Mishima, Chromosomal aberrations, clastogens vs aneugens, Front. Biosci. 9 (2017) 1–16, https://doi.org/10.2741/s468.

[52] V. Savic, B. Yin, N.L. Maas, A.L. Bredemeyer, A.C. Carpenter, B.A. Helmink, K. S. Yang-Lott, B.P. Sleckman, C.H. Bassing, Formation of dynamic g-H2AX domains along broken DNA strands is distinctly regulated by ATM and MDC1 and dependent upon H2AX densities in chromatin, Mol. Cell. 34 (2009) 298–310, https://doi.org/10.1016/j.molcel.2009.04.012.

[53] I.M. Ward, J. Chen, Histone H2AX is phosphorylated in an ATR-dependent manner in response to replicational stress, J. Biol. Chem. 276 (2001) 47759–47762, https://doi.org/10.1074/jbc.C100569200.

[54] N. Nair, M. Shoaib, C.S. Sørensen, Chromatin dynamics in genome stability: roles in suppressing endogenous DNA damage and facilitating DNA repair, Int. J. Mol. Sci. 18 (2017) 1486, https://doi.org/10.3390/ijms18071486.

[55] Y. Li, F.A. Cucinotta, Mathematical model of ATM activation and chromatin relaxation by ionizing radiation, Int. J. Mol. Sci. 21 (2020) 1214, https://doi.org/10.3390/ijms21041214.

[56] D. Strumberg, A.A. Pilon, M. Smith, R. Hickey, L. Malkas, Y. Pommier, Conversion of topoisomerase I cleavage complexes on the leading strand of ribosomal DNA into 5′-phosphorylated DNA double-strand breaks by replication runoff, Mol. Cell. Biol. 20 (2000) 3977–3987, https://doi.org/10.1128/MCB.20.11.3977-3987.2000.

[57] E. Peterson-Roth, M. Reynolds, G. Quievryn, A. Zhitkovich, Mismatch repair proteins are activators of toxic responses to chromium-DNA damage, Mol. Cell Biol. 25 (2005) 3596–3607, https://doi.org/10.1128/MCB.25.9.3596-3607.2005.

[58] M.M. Vilenchik, A.G. Knudson, Endogenous DNA double-strand breaks: production, fidelity of repair, and induction of cancer, Proc. Natl. Acad. Sci. Usa. 100 (2003) 12871–12876, https://doi.org/10.1073/pnas.2135498100.

[59] T. Ohnishi, E. Mori, A. Takahashi, DNA double-strand breaks: their production, recognition, and repair in eukaryotes, Mutat. Res. 669 (2009) 8–12, https://doi.org/10.1016/j.mrfmmm.2009.06.010.

[60] V. Sharma, L.B. Collins, T.H. Chen, N. Herr, S. Takeda, W. Sun, J. Nakamura, Oxidative stress at low levels can induce clustered DNA lesions leading to NHEJ mediated mutations, Oncotarget 7 (2016) 25377, https://doi.org/10.18632/oncotarget.8298.

[61] Y.T. Wang, D.W. Tzeng, C.Y. Wang, J.Y. Hong, J.L. Yang, APE1/Ref-1 prevents oxidative inactivation of ERK for G1-to-S progression following lead acetate exposure, Toxicology 305 (2013) 120–129, https://doi.org/10.1016/j.tox.2013.01.010.

[62] P. Hinhumpatch, P. Navasumrit, K. Chaisatra, J. Promvijit, C. Mahidol, M. Ruchirawat, Oxidative DNA damage and repair in children exposed to low levels of arsenic in utero and during early childhood: application of salivary and urinary biomarkers, Toxicol. Appl. Pharmacol. 273 (2013) 569–579, https://doi.org/10.1016/j.taap.2013.10.002.

[63] J.L. Yang, Y.P. Chen, S.F. Sun, S.D. Chen, NHEJ and BER concurrently repair oxidative DNA damage via initiation of APE1 in rat cortical neurons, lb58-lb58, FASEB J. 31 (2017), https://doi.org/10.1096/fasebj.31.1_supplement.lb58.

[64] L. Passantino, A.B. Muñoz, M. Costa, Sodium metavanadate exhibits carcinogenic tendencies in vitro in immortalized human bronchial epithelial cells, Metallomics 5 (2013) 1357–1367, https://doi.org/10.1039/c3mt00149k.
[65] M.E. Morales, R.S. Derbes, C.M. Ade, J.C. Ortego, J. Stark, P.L. Deininger, A. M. Roy-Engel, Heavy metal exposure influences double strand break DNA repair outcomes, PloS One 11 (2016) e0151367, https://doi.org/10.1371/journal.pone.0151367.
[66] J.R. Whiteside, C.L. Box, T.J. McMillan, S.L. Allinson, Cadmium and copper inhibit both DNA repair activities of polynucleotide kinase, DNA Repair 9 (2010) 83–89, https://doi.org/10.1016/j.dnarep.2009.